Behavioral/Cognitive

The neural dynamics of novel scene imagery

Daniel N. Barry, Gareth R. Barnes, Ian A. Clark, and Eleanor A. Maguire*
Wellcome Centre for Human Neuroimaging, Institute of Neurology,
University College London, London WC1N 3AR

***Corresponding author:** Wellcome Centre for Human Neuroimaging, Institute of Neurology, University College London, 12 Queen Square, London WC1N 3AR, UK
T: +44-20-34484362; F: +44-20-78131445; E: e.maguire@ucl.ac.uk

Abbreviated title: Neural dynamics of scene imagery

Number of pages: 27
Number of figures: 4
Number of tables: 3
Abstract word count: 220
Introduction word count: 641
Discussion word count: 1395

Acknowledgements: This work was supported by a Wellcome Principal Research Fellowship to E.A.M. (101759/Z/13/Z) and the Centre by a Centre Award from Wellcome (203147/Z/16/Z). The authors are grateful to David Bradbury for technical assistance.

The authors declare no competing financial interests.

Abstract

Memory retrieval is characterised by synchronised neural activity between hippocampus and ventromedial prefrontal cortex (vmPFC), with additional evidence that vmPFC activity leads that of the hippocampus. It has been proposed that the mental generation of scene imagery is a crucial component of memory processing. If this is the case, then a comparable interaction between the two brain regions should exist during the construction of novel scene imagery. To address this question, we leveraged the high temporal resolution of magnetoencephalography (MEG) to investigate the construction of novel mental imagery. We tasked male and female humans with imagining scenes and single isolated objects in response to one-word cues. We performed source level power, coherence and causality analyses to characterise the underlying inter-regional interactions. Both scene and object imagination resulted in similar theta power changes in the anterior hippocampus. However, higher theta coherence was observed between the hippocampus and vmPFC in the scene compared to the object condition. Dynamic causal modelling of this interaction revealed that vmPFC drove activity in hippocampus during novel scene construction. These results constitute the first evidence in humans that memory retrieval and scene imagination rely on similar vmPFC-hippocampus neural dynamics. Furthermore, they provide support for theories emphasising similarities between both cognitive processes, and perspectives that propose that the vmPFC guides the construction of context-relevant representations in the hippocampus.

Significance statement

Memory retrieval is characterised by a dialogue between hippocampus and ventromedial prefrontal cortex (vmPFC). It has been proposed that the mental generation of scene imagery is a crucial component of memory processing. If this is the case, then a comparable interaction between the two brain regions should exist during the construction of novel scene imagery. Here, we leveraged the high temporal resolution of magnetoencephalography (MEG), and combined it with a scene imagination task. We found that a hippocampal-vmPFC dialogue existed, and that it took the form of vmPFC driving the hippocampus. We conclude that memory and scene imagination share fundamental neural dynamics, and the process of constructing vivid, spatially coherent, contextually appropriate scene imagery is strongly modulated by vmPFC.

Introduction

Memory formation and retrieval are long-established functions of the hippocampus (Scoville and Milner, 1957). However, cognitive impairments beyond recalling past experiences have been documented following hippocampal damage, including deficits in imagination and future-thinking (Hassabis et al., 2007a; Kwan et al., 2010; Kurczek et al., 2015). Accordingly, contemporary perspectives have converged on a more inclusive account of hippocampal function which accommodates the flexible construction of predictive or fictive representations (Hassabis and Maguire, 2007; Schacter and Addis, 2007; Eichenbaum and Fortin, 2009; Buckner, 2010; Maguire and Mullally, 2013).

One such interpretation, the Scene Construction Theory, proposes that the hippocampus constructs scene imagery to facilitate mental representations, whether recollected or imagined (Hassabis and Maguire, 2007; Maguire and Mullally, 2013). In this context, a scene is defined as a naturalistic three-dimensional spatially coherent representation of the world typically populated by objects and viewed from an egocentric perspective (Maguire and Mullally, 2013; Dalton et al., 2018). In support of this thesis, functional MRI (fMRI) studies have revealed anterior hippocampal recruitment while participants imagined novel scenes (Hassabis et al., 2007b; Zeidman et al., 2015; Zeidman and Maguire, 2016).

However, other regions, including the ventromedial prefrontal cortex (vmPFC), are recruited during (Hassabis et al., 2007b), and seem necessary for (Bertossi et al., 2016a), scene construction. An outstanding question, therefore, is how vmPFC interacts with hippocampus during the generation of scene imagery. The temporal resolution of magnetoencephalography (MEG) renders it a suitable method to address this question. Furthermore, a proposed mechanism of such inter-regional communication is oscillatory coherence (Fries, 2005). Increased theta synchrony between hippocampus and vmPFC has been observed during memory retrieval (Fuentemilla et al., 2014) and

integration (Backus et al., 2016), as well as memory-guided navigation (Kaplan et al., 2014) and decision-making (Guitart-Masip et al., 2013). Demonstrating analogous connectivity during the imagination of novel scenes would provide evidence that memory and scene construction share not only similar loci of brain activity, but are supported by comparable network dynamics.

If oscillatory coherence between hippocampus and vmPFC is evident during scene construction, a question of further relevance concerns the direction of information flow between the two regions. Electrophysiological investigations in rodents, humans and non-human primates have suggested that during initial memory formation, hippocampal activation precedes that of vmPFC (Place et al., 2016). By contrast, retrieval (Place et al., 2016), detection of violations in learned information (Garrido et al., 2015) and subsequent extinction (Lesting et al., 2013), have been characterised by vmPFC driving hippocampus. It is unclear which pattern the generation of novel scene imagery might follow.

Campbell et al. (2018) investigated the directionality of information flow between hippocampus and vmPFC during the imagination of future events using dynamic causal modelling (DCM; Friston et al., 2003) of fMRI data. This revealed a greater influence of hippocampus over vmPFC. However, the temporal resolution of fMRI is not optimal to adequately characterise this dialogue. In contrast, McCormick et al. (2018) recently proposed that vmPFC initiates scene construction. From this perspective, the vmPFC would drive the hippocampus during the imagination of novel scenes.

The current study leveraged the high temporal resolution of MEG to address two questions. First, do hippocampus and vmPFC display coherent activity during the imagination of novel scenes? Given accumulating evidence that theta oscillations mediate the interaction between hippocampus and vmPFC, we predicted an increase in theta coherence between the two regions. Second, does one of these regions exert a stronger influence over the other during scene imagination? In line with the proposal of McCormick et al. (2018), we hypothesised that vmPFC would drive oscillatory activity in

hippocampus. We approached these questions by asking participants to imagine novel scenes (and to imagine single isolated objects as a control condition) in response to single-word cues during MEG. We then used a combination of source localisation techniques measuring power and coherence, as well as DCM for MEG to address the research questions.

Material and Methods

Participants

Twenty-two participants (14 female) took part in this experiment (mean age 27 years; SD 7). Due to the verbal nature of the stimuli, only native English speakers were recruited. Participants gave written informed consent. The University College London Research Ethics Committee approved the study.

Stimuli

Seventy-five scene words and 75 object words were used as stimuli for the imagination task. These comprised a sub-set of the stimuli devised by Clark et al. (2018) for a separate fMRI study. These word categories were closely matched on a number of properties (Table 1) to ensure any differences in neural activity could be solely attributed to the type of mental imagery they evoked. To enable vivid imagination, all words were rated as highly imageable (> 3.5/5). To facilitate the ease with which participants could construct the two different kinds of representations, words were designated as either scene or object-evoking if at least 70% of an independent sample of participants rated them as such (Clark et al., 2018). Additionally, 75 number stimuli were also deployed in a baseline condition involving counting, which were matched to the scene and object words in terms of the number of letters and syllables.

Table 1. Properties of the word stimuli.

Word property		**Word type**			**p-value**	
Lexical criteria	Scene	Object	Number	Scene/Object	Scene/Number	Object/Number
Number of syllables[a]	2.24 (0.87)	2.24 (0.75)	2.24 (0.79)	1	1	1
Number of letters[a]	6.91 (1.95)	6.89 (1.82)	7.03 (2.14)	0.97	0.72	0.68
Number of phonemes[a]	5.83 (1.86)	5.71 (1.64)		0.68		
Number of orthographic neighbours[a]	1.94 (4.16)	2.12 (3.91)		0.81		
Number of phonological neighbours[a]	4.39 (9.76)	4.93 (8.80)		0.72		
Including homophones[a]	4.73 (10.38)	5.16 (9.46)		0.79		
Number of phonographic neighbours[a]	1.01 (2.57)	1.19 (2.65)		0.68		
Including homophones[a]	1.08 (2.84)	1.33 (2.73)		0.58		
Word frequency: Zipf[b]	3.88 (0.70)	3.80 (0.61)		0.46		
Age of acquisition[c]	7.53 (1.98)	7.40 (2.12)		0.70		
Emotional constructs						
Valence[d]	5.79 (1.11)	5.73 (1.07)		0.74		
Number of positive words[d,e]	60 (80%)	62 (83%)		0.86		
Hedonic valence[d,f]	1.15 (0.73)	1.09 (0.69)		0.62		
Arousal[d]	4.16 (0.96)	4.10 (0.95)		0.68		
Imagery						
Concreteness[g]	4.67 (0.19)	4.67 (0.24)		0.87		
Imageability[h]	4.44 (0.26)	4.41 (0.32)		0.57		

Means (standard deviations). Two-tailed p-values for t-tests (χ^2 test for the number of positive words). Note that each comparison was assessed separately in order to provide a greater opportunity for any differences between conditions to be identified.

[a]From the English Lexicon Project (Balota et al. (2007): exlexicon.wustl.edu).

[b]From van Heuven et al. (2014). The Zipf scale is a standardised measure of word frequency using a logarithmic scale. Values go from 1 (low frequency words) to 6 (high frequency words).

[c]From Kuperman et al. (2012).

[d]From Warriner et al. (2013).

[e]Positive words were those that had a valence score greater than or equal to 5.

[f]Hedonic valence is the distance from neutrality (i.e., from 5), regardless of being positive or negative, as per Vigliocco et al. (2014).

[g]From Brysbaert et al. (2014).

[h]From Clark et al. (2018).

181 **Experimental design of the task**

182 Prior to the MEG scan, participants received task instructions and practiced for the equivalent of two
183 in-scanner sessions. In the MEG scanner, experimental stimuli were delivered aurally via MEG-
184 compatible earbuds using the Cogent toolbox (www.vislab.ucl.ac.uk/cogent.php), running in
185 MATLAB (version 2012).

186

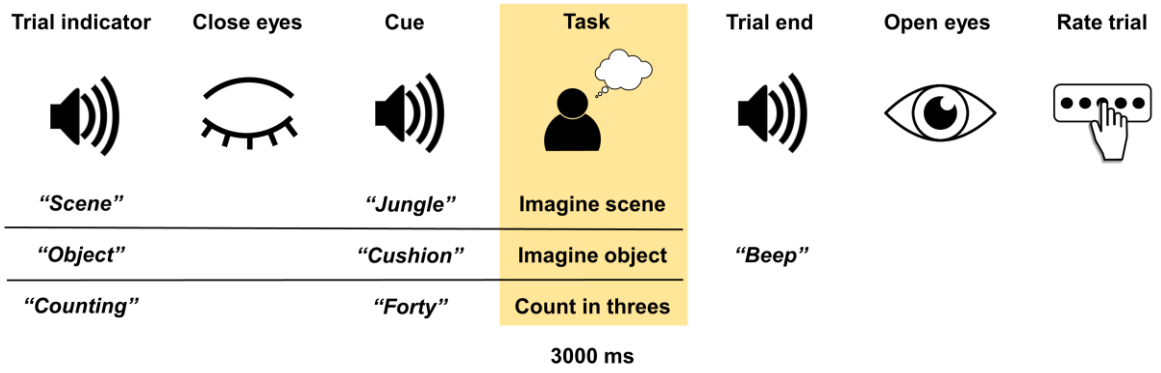

187

188 **Figure 1. Trial structure.** The task period selected for analysis is highlighted.

189

190 To prepare participants for each trial type, participants first heard either the word "scene", "object"
191 or "counting" (Figure 1). This was intended to minimise category confusion during the scene and
192 object trials. Participants immediately closed their eyes and waited for an auditory cue which
193 followed a jittered duration of between 1300 and 1700 milliseconds. During scene trials,
194 participants constructed a novel, vivid scene from their imagination, based on the cue (e.g. "jungle").
195 During object imagery, participants imagined a single novel object (e.g. "cushion") against a white
196 background. Counting trials involved mentally counting in threes from a number cue (e.g. "forty").
197 The task periods were 3000 ms in duration. Participants then heard a beep and opened their eyes.
198 They were presented with a rating screen. For scene and object trials, they were asked "What did
199 you imagine?" If they failed to perform the task, they selected "unsuccessful". Otherwise, they could
200 select "low detail scene", "high detail scene", "low detail object" or "high detail object". This allowed
201 participants to indicate both the level of detail present in the mental imagery, and also to reclassify

scene and object trials if they had inadvertently imagined an object as a scene or vice versa. For counting trials, participants were asked “How well did you concentrate?” on a scale from 1 (not at all) to 5 (extremely well). Following this was a 1000 ms delay before the next trial. There were eight scanner sessions in total, seven containing nine stimuli from each condition in a random order, and one final session with 12 stimuli from each condition. Eighteen participants completed all eight sessions; the remaining four participants completed seven sessions.

Post-scan recognition memory test

After the scan, participants took part in a recognition memory test. Participants were not informed about this test prior to the scan to avoid confounding the imagination task with attempts to memorise the stimuli. They were presented with scene and object words, and asked if the word was previously presented in the scanner or not. The available response options were “yes” or “no”. Alongside the 75 scene and 75 object words which had been presented in the scanner, there were 38 scene and 38 object foils; the presentation was randomised for each participant. The scene and object foil words were also matched to the words presented in the scanner on the characteristics outlined in Table 1.

Statistical analysis: behavioural data

Word properties

Comparisons between word category properties were performed using independent sample t-tests in the case of continuous variables and chi squared tests for categorical variables. Significance was determined at an alpha level of $p < 0.05$. Statistical analyses were performed using SPSS statistical package version 22 (SPSS, Chicago, IL).

In-scanner ratings

Comparison of the percentage of successful trials in each condition was performed using a repeated-

228 measures one-way ANOVA. These percentages accommodate participants' reclassifications of
229 scenes and objects during task performance. Greenhouse–Geisser adjustment to the degrees of
230 freedom was applied if Mauchly's sphericity test detected a violation of sphericity. Comparison of
231 trial reclassifications, and highly detailed ratings were performed using paired samples t-tests.
232
233 ***Post-scan recognition memory test***
234 To ensure a relevant comparison with trials used in the MEG analysis, only successfully completed
235 trials in the scanner were included as target stimuli in this analysis, and stimuli were reclassified as
236 scenes or objects if the individual participant had imagined them as such during the task.
237 Comparison of the percentage of correctly recognised scenes and objects, and d' values were
238 performed using paired samples t-tests.
239
240 **MEG recording and preprocessing**
241 A CTF Omega whole-head MEG system with 273 functioning second order gradiometers recorded
242 data at a sample rate of 1200Hz. Four EOG electrodes were used to measure a participant's vertical
243 and horizontal eye movements. To rule out the possibility that differences between conditions in
244 subsequent analyses were related to differences in eye movements, we computed the variance of
245 these two EOG signals during each trial, which served as an indirect measure of saccadic activity.
246 These variances were averaged across trials within each condition and normalised within subjects so
247 that values for the three conditions summed to 1. A 1x3 repeated measures ANOVA did not detect
248 any differences in eye movements between conditions ($F_{(2,42)} = 1.12$, $p = 0.335$). Data were epoched
249 into 3 second mental imagery and counting periods, baseline corrected, and concatenated across
250 sessions.
251
252 **Statistical analysis: MEG data**
253 All MEG analyses were performed using SPM12 (www.fil.ion.ucl.ac.uk/spm). Source reconstruction

254 was performed using the SPM DAISS toolbox (https://github.com/spm/DAiSS).

255

256 ***MEG source reconstruction***

257 To estimate differences in power between experimental conditions in source space, the Linearly
258 Constrained Minimum Variance (LCMV) beamformer was used. This filter uses a series of weights to
259 linearly map MEG sensor data into source space to estimate power at a particular location, while
260 attenuating activity from other sources. For each participant, a single set of filter weights was
261 constructed based on the data from all three conditions within the 4-8Hz band and a 0-3000 ms peri-
262 stimulus window. Analysis was performed in MNI space using a 5 mm grid and coregistration was
263 based on nasion, left and right preauricular fiducials. Co-registration and the forward model were
264 computed using a single-shell head model (Nolte, 2003). Power was estimated in the theta (4-8Hz)
265 frequency band and the 0-3000 ms time window, with one power image per condition being
266 generated for each participant. These images were smoothed using a 12 mm Gaussian kernel and
267 entered into a second-level random effects (1x3) ANOVA in SPM to investigate power differences
268 across conditions. Small volume correction was performed using a bilateral hippocampus mask
269 generated from the AAL atlas implemented in the WFU PickAtlas software
270 (http://fmri.wfubmc.edu/software/pickatlas). Identification of activation peaks in other regions was
271 performed using the AAL atlas (Tzourio-Mazoyer et al., 2002).

272

273 ***Coherence***

274 Coherent activity between sources was measured using the Dynamic Imaging of Coherent Sources
275 (DICS) approach (Gross et al., 2001). In this case, a beamformer reference signal estimate is first
276 performed for a reference location, in this case a defined source in the anterior hippocampus. This
277 analysis was again based on a 4-8Hz band within the 3000 ms task time window. Then scanning the
278 brain on a 3 mm grid, a signal estimate was made at each location and the coherence between this
279 signal and the reference (in the 4-8Hz band) computed. These values are output as an image for

280 each condition which represents a brain-wide map of coherent activity with the reference source.
281 These images were smoothed using a 12 mm Gaussian kernel, and contrasts between conditions at
282 the group level were performed using a second-level random effects paired t-test in SPM. For
283 subsequent directional causality analysis, time series of theta activity during the 3000 ms imagery
284 task period were extracted from two 10 mm radius spheres encompassing the hippocampal
285 reference source and the group coherence peak in the vmPFC using the LCMV beamforming
286 algorithm.
287
288 ***Effective connectivity***
289 To determine effective connectivity, we utilised DCM for Cross Spectral Densities (Moran et al.,
290 2009), which analyses the magnitude of cross spectra between regions. The DCM approach involves
291 creating a model specifying the direction of inter-regional information flow and fitting this model to
292 the actual neural data. Multiple possible models can be generated and compared in the same
293 manner to ascertain the best explanation for the experimental observations. DCM for MEG uses a
294 biophysical neural-mass model which attempts to summarise the activity of millions of neurons
295 within a region. This model accommodates different neuronal types and their intrinsic connectivity,
296 treating the measurable output of these cell populations as a convolution of their input. If a region
297 is being causally influenced by another, this activity should change in a predictable manner based on
298 the nature of afferent input from the source. These inputs are characterised as forward, or "bottom
299 up", if they project to the middle layers of the cortex, backward, or "top down" if they target deep
300 and superficial layers, or lateral if they innervate all layers (Felleman and Van Essen, 1991). One can
301 therefore test biologically plausible models based on known structural connections between two
302 regions, which differ in terms of which connections are functionally modulated by the experimental
303 task.
304
305 The DCM estimation process attempts to fit these different models to the observed data as closely

as possible by tuning their parameters. The evidence for any one model represents a balance between how accurate and parsimonious it is in explaining the data, as models with too many parameters are penalised. In this study, we used a convolution-based local field potential (LFP) neuronal model, as this is the simplest and most efficient approach when addressing hypotheses regarding differences in effective extrinsic connectivity (Moran et al., 2013). To assess which model best explains the observed data on a group level, random effects Bayesian model comparison (Stephan et al., 2009) is performed, which compares the evidence for each model across all participants, and generates the probability of it being the winning model.

Results

Behavioural

In-scanner task performance

Participants' in-scanner self-rated performance was high (Table 2), with a minimal proportion of trials rated as unsuccessful. Of the trials eligible for subsequent analysis, there was a similar proportion of scene imagery, object imagery and counting trials ($F_{(1.22,25.64)} = 2.25$, $p = 0.142$). Scene and object stimuli appeared to successfully evoke the intended mental imagery, as a comparably low percentage of trials were reclassified in the two conditions ($t_{(21)} = -1.67$, $p = 0.110$). The majority of scenes and objects were imagined in high detail with both conditions matched on this rating ($t_{(21)} = -1.33$, $p = 0.199$). Furthermore, for most counting trials, concentration was rated as high (>3/5), indicating participants successfully maintained their attention during this baseline condition.

Table 2. Scanner trial ratings.

	Condition				p-value
	Scene	Object	Counting	Unsuccessful	Scene/Object/Counting
Proportion of total trials (%)	32.56 (2.51)	31.03 (2.90)	32.28 (1.24)	4.13 (3.10)	0.142
Reclassified trials (%)	As Object	As Scene			Scene/Object
	3.03 (3.01)	5.78 (8.15)			0.110
					Scene/Object
High detail (%)	71.41 (13.79)	74.70 (12.71)			0.199
High concentration (%)			78.09 (7.91)		

Table 3. Post-scan recognition memory performance and d' values for scenes and objects.

	Condition		p-value (vs 50% chance)		p-value (Scene vs Object)
	Scene	Object	Scene	Object	
Correct recognition (%)	85.67 (2.94)	88.35 (2.47)	<0.001	<0.001	0.048
d'	2.92 (1.26)	4.02 (1.28)			<0.001

363 ***Post-scan recognition memory test***

364 Participants were able to correctly recognise most of the scene and object stimuli that they
365 previously imagined in the scanner, performing significantly above chance level in both conditions
366 (Table 3). They remembered a greater proportion of objects than scenes ($t_{(21)} = -2.10$, $p = 0.048$). In
367 addition, d' scores indicated that participants were significantly less accurate in distinguishing
368 between new and old scene compared to object words ($t_{(21)} = -4.19$, $p < 0.001$). Superior memory for
369 objects corroborates the findings of Clark et al. (2018), and implies that a greater power change or
370 heightened connectivity during scene imagination relative to object imagination could not be
371 attributable to better encoding of scenes.

372

373 **MEG**

374 ***Theta power changes during mental imagery***

375 We first determined which brain regions were active during imagination in general, that is, scene
376 and object imagination tasks combined compared to the low-level counting condition. Due to the
377 obvious disparity in task demands between the imagery and baseline conditions, we used a
378 conservative whole brain family-wise error corrected threshold of $p < 0.001$. A widespread change in
379 theta power was observed during mental imagery when compared to the baseline task (Figure 2).
380 This was evident throughout the left anterior temporal lobe, with an activation peak at the whole-
381 brain level in the inferior frontal gyrus (x = -38; y = 24, z = -4; Z-score = 6.23). Our primary *a priori*
382 region of interest was the anterior hippocampus, where a significant change from baseline was also
383 observed. A subsequent t-contrast revealed the observed changes represented an attenuation of
384 theta power during imagination rather than an increase from baseline. Nonetheless, we regarded
385 these power changes as an indication of task-related neural activity, and for subsequent connectivity
386 analyses we did not exclude the possibility of inter-regional coherence in the presence of lower
387 power. Subsequent small volume correction revealed an overall peak (-32, -4, -28; Z = 5.82) and sub-
388 peak (-32, -6, -22; Z = 5.61) in the left anterior hippocampus.

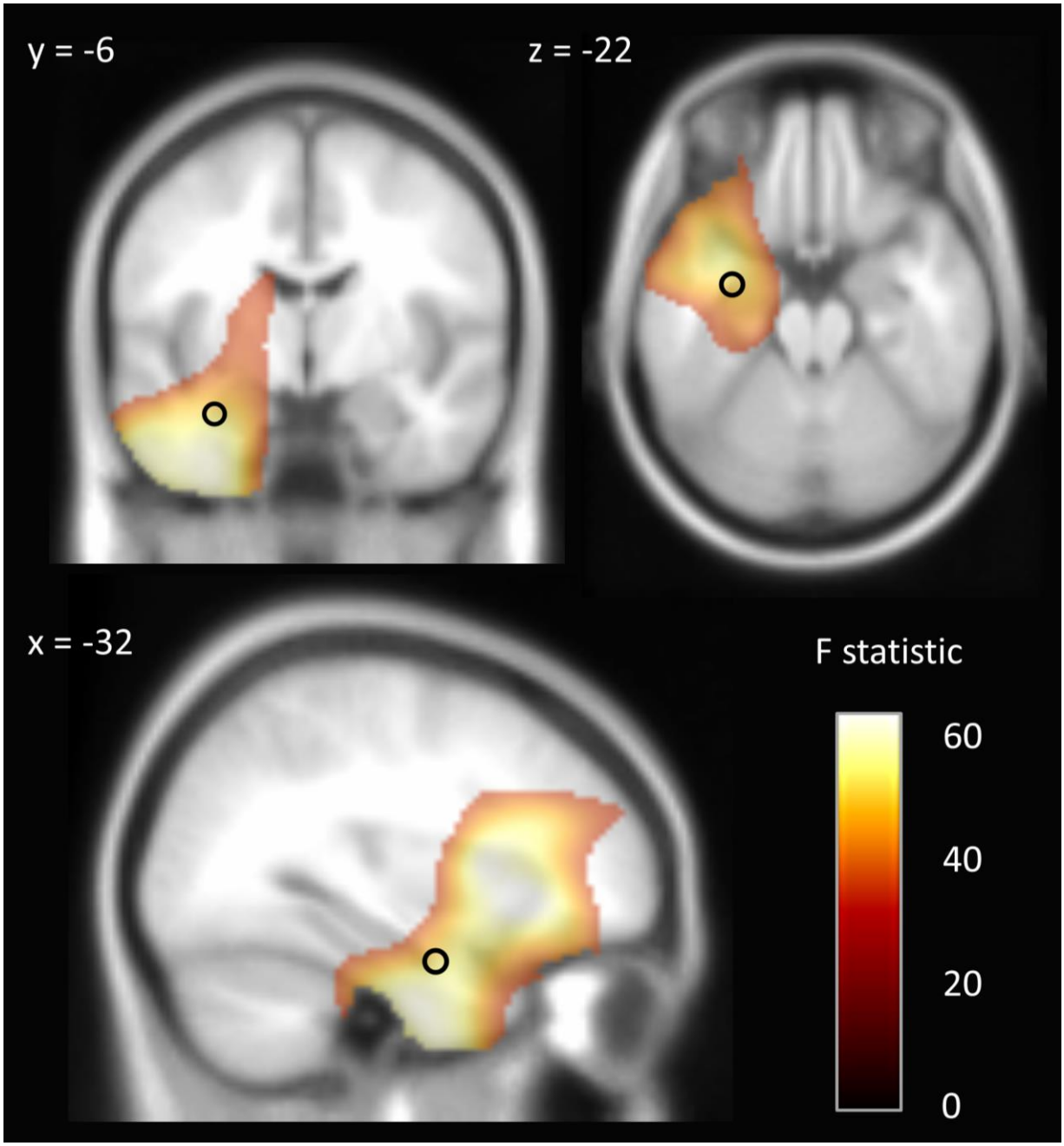

Figure 2. MEG source reconstruction of theta (4-8 Hz) power changes during mental imagery (scenes and objects) compared to the baseline condition. The black circle represents the peak location in anterior hippocampus used for subsequent connectivity analyses. Images are FWE thresholded at $p < 0.001$ and superimposed on the Montreal Neurological Institute (MNI) 152 T1 image.

As the overall hippocampal peak closely bordered the perirhinal cortex and fusiform gyrus, the more dorsal and posterior sub-peak (Figure 2, black circle) was selected for connectivity analyses in order to be confident that source-localised activity originated from the hippocampus. Of note, no difference in theta power was observed at the whole brain level between scene and object

imagination, even using an exploratory uncorrected threshold of $p < 0.005$ (cluster size > 5), or within the hippocampus in an ROI analysis ($p < 0.05$ uncorrected). In summary, scene and object imagery appeared to engage a common network of brain regions to a similar degree, including the anterior hippocampus. Therefore, any observed differences in connectivity between the two imagery conditions could not be explained by differences in power. Consequently, in the subsequent analyses, we were able to directly explore the changes in network connectivity due to imagining scenes rather than single objects.

Hippocampal connectivity during scene imagery

Having established a peak location of power changes in the anterior hippocampus during mental imagery, we then sought to investigate whether the imagination of scenes was associated with greater connectivity with any other regions of the brain when compared to object imagination. We found higher theta coherence in the left fusiform gyrus (Figure 3 upper panel; peak voxel: -32, -18, -32; $Z = 3.58$, $p < 0.001$ uncorrected) and parahippocampal cortex (peak voxel: -32, -38, -14; $Z = 3.47$, $p < 0.001$ uncorrected) during scene imagery.

Given that we had a specific *a priori* hypothesis regarding connectivity between the hippocampus and vmPFC for scene imagery, we applied an uncorrected threshold of $p < 0.005$, and discovered a bilateral cluster of voxels coherent with the hippocampal source, at the most ventral extent of the vmPFC (Figure 3 lower panel; peak voxel: 18, 34, -16; $Z = 2.87$), with a sub-peak in the left vmPFC (-2, 46, - 28; $Z = 2.86$). This left-sided vmPFC peak was used for subsequent anatomically-informed analyses of effective connectivity as the hippocampus and vmPFC are connected ipsilaterally. Of note, the reverse contrast (greater connectivity for objects than scenes) did not reveal any significant results throughout the whole brain at a significance level of $p < 0.005$.

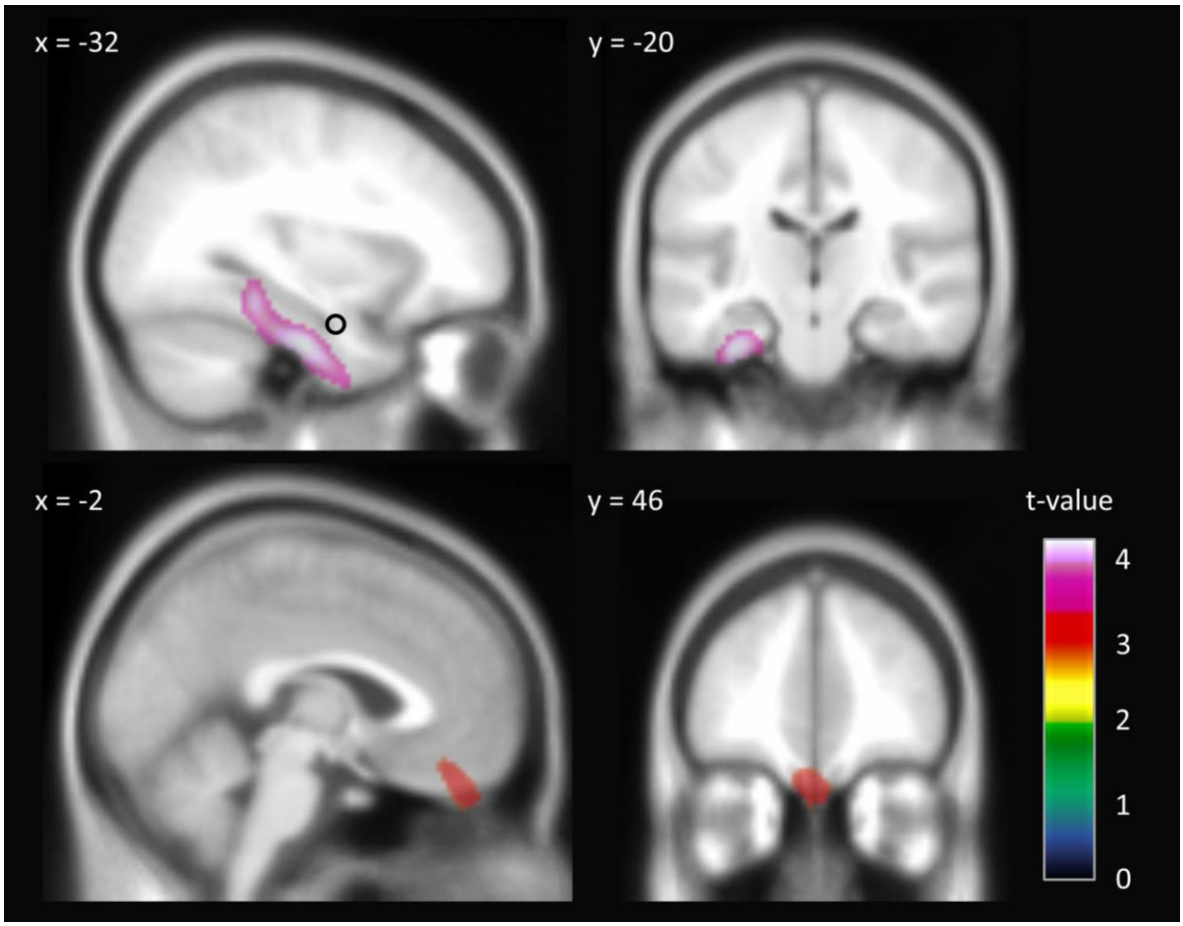

Figure 3. Brain areas displaying higher theta coherence with the left anterior hippocampus during scene imagination compared to object imagination. The fusiform and parahippocampal cortices (upper panel, display thresholded at $p < 0.001$ uncorrected, superimposed on the MNI 152 T1 image), and the vmPFC (lower panel, $p < 0.005$ uncorrected) showed higher coherence with the hippocampal source (black circle). No areas showed higher theta coherence with the hippocampus for object over scene imagery.

Effective connectivity during scene imagery

Having established higher theta coherence between hippocampus and vmPFC during scene imagination, we then investigated the directionality of information flow between the two regions. Using DCM for Cross Spectral Densities, we first specified a biologically plausible model of hippocampal-vmPFC connectivity. As the anterior hippocampus projects directly to the middle layers of the ventral extent of the ipsilateral vmPFC (where we observed high theta coherence) via the fornix (Aggleton et al., 2015), we designated this connection as forward. Because return

443 projections are indirectly channeled through the entorhinal cortex (EC), vmPFC influence over the
444 hippocampus is best characterised by the pattern of laminar innervation in EC. vmPFC efferents
445 terminate in all layers of EC (Rempel-Clower and Barbas, 2000), and consequently we designated the
446 return connection as lateral (Felleman and Van Essen, 1991). Additional thalamic relays exist
447 between the two structures (Varela et al., 2014; Xiao et al., 2009) but are not considered here as the
448 hierarchical nature of this connection type is unclear (Bastos et al., 2012).
449
450 Of key interest was the predominant direction of information flow between hippocampus and
451 vmPFC during scene imagination. Therfore we proposed two anatomically informed models. In
452 model 1, hippocampal activity drove the vmPFC via its forward connection. In model 2, lateral
453 projections from the vmPFC modulated activity of the hippocampus (Figure 4A). In both models,
454 object imagination was used as the baseline. The specified time period was the 3000 ms imagination
455 task, and analysis of cross spectral density was constrained to the theta (4-8Hz) frequency band to
456 retain consistency with previous power and coherence analyses. We applied both models to the
457 observed data, and subsequently performed Bayesian model comparison to determine which model
458 was most likely to explain the relationship between the two regions. The model most likely to be the
459 winning model across all subjects, with a probability of 91.54%, was the vmPFC exerting a causal
460 influence over the anterior hippocampus during the imagination of novel scenes (Figure 4B).
461

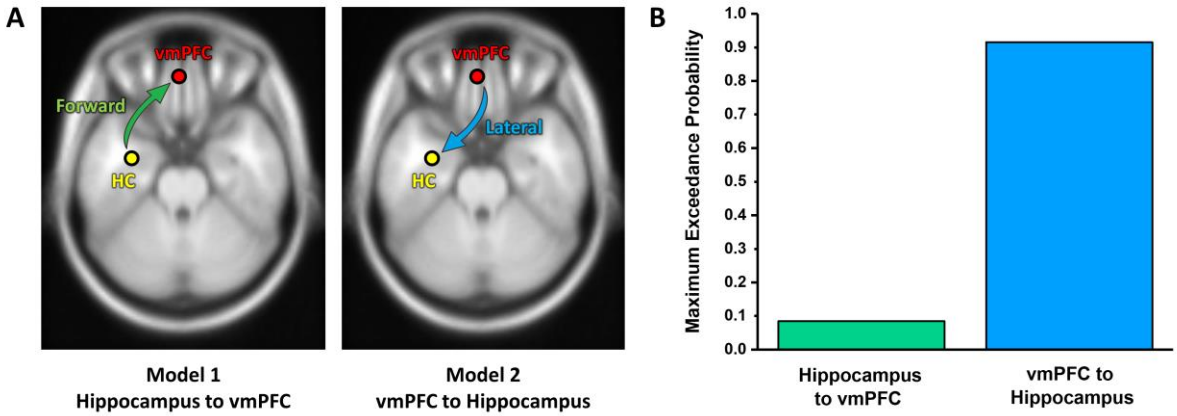

Figure 4. Dynamic Causal Modelling of the interaction between the hippocampus and vmPFC. *A*, Two proposed models of effective connectivity between the coherent peaks in hippocampus and vmPFC. ***B***, Results of Bayesian Model Comparison indicated a stronger influence of the vmPFC on hippocampal activity during scene imagination.

Discussion

The aim of this study was to investigate whether the imagination of novel scenes is supported by a hippocampal-vmPFC dialogue. We found that engaging in mental imagery, whether spatially coherent scenes or isolated objects, resulted in comparable theta power decreases in the left hippocampus. However, theta coherence between the anterior hippocampus and vmPFC was significantly higher for scene imagination compared to object imagination. In addition, dynamic causal modelling of this interaction revealed the vmPFC drove hippocampal activity during the scene construction process.

These findings corroborate previous fMRI studies demonstrating that the anterior, rather than posterior, hippocampus contributes to the mental construction of novel scene imagery (Hassabis et al., 2007b; Zeidman et al., 2015; Zeidman and Maguire, 2016, Dalton et al., 2018). An interesting feature of our data, which contradicts some previous reports of theta increases during learning and memory tasks, is the attenuation of this frequency during imagination. However, there is accumulating evidence from electroencephalography (EEG; Fellner et al., 2016) and MEG (Guderian et al., 2009) demonstrating a strong decrease in medial temporal lobe theta during memory

encoding. These findings have been validated using direct intracranial recordings in humans, with brain-wide decreases in theta power predicting subsequent recall (Burke et al., 2013; Greenberg et al., 2015), and specifically in the hippocampus (Sederberg et al., 2007; Lega et al., 2012; Matsumoto et al., 2013; Lega et al., 2017). A decrease in 8Hz power has also been reported during memory retrieval (Michelmann et al., 2016). Furthermore, decreases in low frequency power appear to be negatively correlated with the fMRI BOLD response (Fellner et al., 2016; Scheeringa et al., 2011), and, therefore, our findings may be consistent with observed BOLD increases in previous fMRI studies.

The functional significance of the observed theta power decrease is not yet clear. However, in rodents, reduced hippocampal theta power is observed upon introduction to a novel or unexpected environment (Jeewajee et al., 2008). Our task involved the rapid mental construction of novel scenes (and so environments) in response to unpredictable stimuli, and the underlying oscillatory dynamics may, therefore, be similar. Importantly, a lower amplitude signal can still contain rich information about the underlying mental representations during memory retrieval (Michelmann et al., 2016).

In the current study, theta power in the hippocampus did not differentiate between scene and object imagination. This accords with recent fMRI findings showing that object stimuli engage the hippocampus (Clark et al., 2018; Dalton et al., 2018), and that there may be different circuits within the hippocampus, each associated with different cortical inputs, which become engaged depending on the nature of the stimuli and the task at hand. In a similar vein, Fuentemilla et al. (2014) demonstrated that while hippocampal theta power was similar during the retrieval of semantic and autobiographical memories, connectivity with the vmPFC was higher during the latter hippocampal-dependent task. Accordingly, we observed increased theta coherence between the anterior hippocampus and vmPFC during scene construction moreso than object construction, indicating a similar network dynamic may support memory retrieval and scene imagination.

How might the vmPFC facilitate both processes? The vmPFC is a proposed target of systems-level memory consolidation and long-term storage (Nieuwenhuis and Takashima, 2011), with evidence in humans of the reactivation of specific remote memory traces (Bonnici et al., 2012; Barry et al., 2018). Yet participants in the current study were instructed to avoid recalling a specific memory during the imagination process. However, the vmPFC is also thought to slowly extract regularities across past experiences to form superordinate representations, or schemas (van Kesteren et al., 2013; Gilboa and Marlatte, 2017). These may serve as flexible conceptual "templates" within which to rapidly and efficiently construct spatially coherent novel scenes in concert with the hippocampus.

Patients with vmPFC damage have schema-related deficits (Ciaramelli et al. 2006; Gilboa et al, 2006; Ghosh et al., 2014; Warren et al., 2014) and are impaired at constructing scene imagery (Bertossi et al., 2016a; Bertossi et al., 2016b; Bertossi et al., 2017; De Luca et al., 2018). However, such patients can generate imagery for indivdual scenes from autobiographical events in response to highly specific cues (Kurczek et al., 2015). Consequently, and in keeping with its role in supporting schema, it has been suggested that the vmPFC is necessary to select appropriate elements for a particular scene, while the hippocampus is needed to construct the scene imagery (McCormick et al., 2018).

An ensuing question is how the two brain regions collaborate to produce these integrated representations. One interpretation is that during imagination, the role of the vmPFC is to fuse distributed knowledge into a novel representation (Benoit et al., 2014), with corresponding evidence from fMRI that the hippocampus drives activity in the vmPFC when simulating the future (Campbell et al., 2018). However, an alternate perspective, as alluded to above, holds that the vmPFC exerts direct control over the hippocampus to select context-relevant representations (Eichenbaum, 2017; McCormick et al., 2018). Our finding of vmPFC exerting a causal influence over the hippocampus during scene imagination is more consistent with this latter view. We also regard MEG as a method

536 well-suited to characterising this relationship given that it is a direct and time-resolved measure of
537 neural activity. What aspects of the lateral projection from vmPFC are influencing the hippocampus
538 remains an open question. The preferential termination of neurons in the middle layers of the
539 entorhinal cortex (Rempel-Clower and Barbas, 2000) indicates the presence of a driving and
540 excitatory input (Bastos et al., 2012) to the hippocampus. Conversely, the majority of residual
541 connections project to inhibitory neurons in the deepest layers (Joyce and Barbas, 2018), suggesting
542 vmPFC also heavily constrains hippocampal output. From a behavioural perspective, the inability of
543 patients with vmPFC damage to retrieve context-relevant information during scene construction
544 tasks (Bertossi et al., 2016a) – which involve cues that are relatively unconstrained (Hassabis et al.,
545 2007a) – while being also unable to suppress context-irrelevant information while confabulating
546 (Turner et al., 2008), suggests the vmPFC may control both hippocampal input and output during
547 scene imagination.
548
549 Our results also revealed that engaging in mental imagery in response to scene and object words
550 relative to the counting baseline resulted in power decreases in the left inferior frontal gyrus. This
551 activation peak was localised to Brodmann Area 47, a region implicated in the processing of verbal
552 stimuli (Krieger-Redwood et al., 2015), in particular single words (Cutting et al., 2006). As this
553 activation was common to scene and object words, it likely reflects the increased demands in
554 semantic processing relative to the number stimuli in the baseline counting condition. This lexical
555 processing is likely to be contemporaneous with mental imagery (Lewis and Poeppel, 2014), and it is
556 therefore unlikely that word comprehension and imagination in the current experiment are
557 temporally dissociable.
558
559 One additional finding which differentiated scene from object construction was increased theta
560 coherence between the anterior hippocampus and the fusiform and parahippocampal cortices.
561 Increased fusiform activity has also been observed in a separate fMRI study involving the scene word

stimuli used in the current experiment (Clark et al., 2018). This region appears to represent diverse categories of objects, living beings and their interactions (Grill-Spector et al., 2006; Cukur et al., 2013), and scenes represent the coherent integration of these constituent elements. Observed coherence with the parahippocampal cortex during scene imagination is consistent with the parahippocampal cortex's proposed role in processing scenes (Epstein, 2008; Mullally and Maguire, 2011). This connectivity profile, therefore, suggests that the anterior hippocampus may be a convergence zone for appropriate object categories and their interaction within a defined space, permitting the generation of scene imagery (Dalton and Maguire, 2017).

In summary, our results characterise, for the first time, a core neural dynamic which underlies scene construction, a process held by some to be fundamental to key cognitive functions including episodic memory and future-thinking. Previous studies have demonstrated co-activation of (Hassabis et al., 2007b), and a dependency on (Hassabis et al., 2007a; Bertossi et al., 2016a), the hippocampus and vmPFC during scene construction. By leveraging the high temporal resolution of MEG, we have extended these findings to demonstrate their functional connectivity during this process. Furthermore, we have shown that the direction of information flow during scene imagination mirrors that observed during memory retrieval (Place et al., 2016), with vmPFC driving hippocampal activity. We conclude that memory and imagination share fundamental neural dynamics, and the process of constructing vivid, spatially coherent, contextually appropriate scene imagery is strongly modulated by the vmPFC.

References

Aggleton JP, Wright NF, Rosene DL, Saunders RC (2015) Complementary patterns of direct amygdala and hippocampal projections to the macaque prefrontal cortex. Cereb Cortex 25:4351-4373.

Backus A, Schoffelen JM, Szebenyi S, Hanslmayr S., Doeller C F (2016) Hippocampal-prefrontal theta oscillations support memory integration. Curr Biol 26:450-457.

Balota DA, Yap MJ, Hutchison KA, Cortese MJ, Kessler B, Loftis B, Neely JH, Nelson DL, Simpson GB, Treiman R (2007) The english lexicon project. Behav Res Methods 39:445-459.

590 Barry DN, Chadwick MJ, Maguire EA (2018) Nonmonotonic recruitment of ventromedial prefrontal
591 cortex during remote memory recall. PLoS Biol 16:e2005479.
592 Bastos AM, Usrey WM, Adams RA, Mangun GR, Fries P, Friston KJ (2012) Canonical microcircuits for
593 predictive coding. Neuron 76:695-711.
594 Benoit RG, Szpunar KK, Schacter DL (2014) Ventromedial prefrontal cortex supports affective future
595 simulation by integrating distributed knowledge. Proc Natl Acad Sci U S A 111:16550-16555.
596 Bertossi E, Aleo F, Braghittoni D, Ciaramelli E (2016a) Stuck in the here and now: Construction of
597 fictitious and future experiences following ventromedial prefrontal damage.
598 Neuropsychologia 81:107-116.
599 Bertossi E, Tesini C, Cappelli A, Ciaramelli E (2016b) Ventromedial prefrontal damage causes a
600 pervasive impairment of episodic memory and future thinking. Neuropsychologia 90:12-24.
601 Bertossi E, Candela V, De Luca F, Ciaramelli E (2017). Episodic future thinking following vmPFC
602 damage: Impaired event construction, maintenance, or narration? Neuropsychology 31:337-
603 348.
604 Bonnici HM, Chadwick MJ, Lutti A, Hassabis D, Weiskopf N, Maguire EA (2012) Detecting
605 representations of recent and remote autobiographical memories in vmPFC and
606 hippocampus. J Neurosci 32:16982-16991.
607 Brysbaert M, Warriner AB, Kuperman V (2014) Concreteness ratings for 40 thousand generally
608 known English word lemmas. Behav Res Methods 46:904-911.
609 Buckner RL (2010) The role of the hippocampus in prediction and imagination. Annu Rev Psychol 27-
610 48:C21-28.
611 Burke JF, Zaghloul KA, Jacobs J, Williams RB, Sperling MR, Sharan AD, Kahana MJ (2013) Synchronous
612 and asynchronous theta and gamma activity during episodic memory formation. J Neurosci
613 33:292-304.
614 Campbell KL, Madore KP, Benoit RG, Thakral PP, Schacter DL (2018) Increased hippocampus to
615 ventromedial prefrontal connectivity during the construction of episodic future events.
616 Hippocampus 28:76-80.
617 Ciaramelli E, Ghetti S, Frattarelli M, Ladavas E (2006) When true memory availability promotes false
618 memory: evidence from confabulating patients. Neuropsychologia 44:1866-1877.
619 Clark IA, Kim M, Maguire EA (2018) Verbal paired associates and the hippocampus: the role of
620 scenes. J Cogn Neurosci (in press: doi: 10.1162/jocn_a_01315).
621 Cukur T, Huth AG, Nishimoto S, Gallant JL (2013) Functional subdomains within human FFA. J
622 Neurosci 33:16748-16766.
623 Cutting LE, Clements AM, Courtney S, Rimrodt SL, Schafer JG, Bisesi J, Pekar JJ, Pugh KR (2006)
624 Differential components of sentence comprehension: beyond single word reading and
625 memory. Neuroimage 29:429-438.
626 Dalton MA, Maguire EA (2017) The pre/parasubiculum: a hippocampal hub for scene-based
627 cognition? Curr Opin Behav Sci 17:34-40.
628 Dalton MA, Zeidman P, McCormick C, Maguire, EA (2018) Differentiable processing of objects,
629 associations and scenes within the hippocampus. J Neurosci 38:8146-8159.
630 de Borst, AW, Sack AT, Jansma BM, Esposito F, de Martino F, Valente G, Roebroeck A, di Salle F,
631 Goebel R, Formisano, E (2012) Integration of “what” and “where” in frontal cortex during
632 visual imagery of scenes. Neuroimage 60:47-58.
633 De Luca F, McCormick C, Mullally SL, Intraub H, Maguire EA, Ciaramelli E (2018) Boundary extension
634 is attenuated in patients with ventromedial prefrontal cortex damage. Cortex 108:1-12.
635 Eichenbaum H (2017) Prefrontal-hippocampal interactions in episodic memory. Nature Rev Neurosci
636 18:547-558.
637 Eichenbaum H, Fortin NJ (2009) The neurobiology of memory based predictions. Philos Trans R Soc B
638 364:1183-1191.
639 Epstein RA (2008) Parahippocampal and retrosplenial contributions to human spatial navigation.
640 Trends Cogn Sci 12:388-396.

Felleman DJ, Van Essen DC (1991) Distributed hierarchical processing in the primate cerebral cortex. Cereb Cortex 1:1-47.

Fellner MC, Volberg G, Wimber M, Goldhacker M, Greenlee MW, Hanslmayr S (2016) Spatial mnemonic encoding: Theta power decreases and medial temporal lobe BOLD increases co-occur during the usage of the method of loci. eNeuro 3:e0184-16.2016.

Fries P (2005). A mechanism for cognitive dynamics: neuronal communication through neuronal coherence. Trends Cogn Sci 9:474-480.

Friston KJ, Harrison L, Penny W (2003) Dynamic causal modelling. Neuroimage 19:1273-1302.

Fuentemilla L, Barnes GR, Duzel E, Levine B (2014) Theta oscillations orchestrate medial temporal lobe and neocortex in remembering autobiographical memories. Neuroimage 85:730-737.

Garrido MI, Barnes GR, Kumaran D, Maguire EA, Dolan RJ (2015) Ventromedial prefrontal cortex drives hippocampal theta oscillations induced by mismatch computations. Neuroimage, 120:362-370.

Ghosh VE, Moscovitch M, Melo Colella B, Gilboa A (2014) Schema representation in patients with ventromedial PFC lesions. J Neurosci 34:12057-12070.

Gilboa A, Alain C, Stuss DT, Melo B, Miller S, Moscovitch M (2006) Mechanisms of spontaneous confabulations: a strategic retrieval account. Brain 129:1399-1414.

Gilboa A, Marlatte H (2017) Neurobiology of schemas and schema-mediated memory. Trends Cogn Sci 21:618-631.

Greenberg JA, Burke JF, Haque R, Kahana MJ, Zaghloul KA (2015) Decreases in theta and increases in high frequency activity underlie associative memory encoding. Neuroimage 114:257-263.

Grill-Spector K, Sayres R, Ress D (2006) High-resolution imaging reveals highly selective nonface clusters in the fusiform face area. Nat Neurosci 9:1177.

Gross J, Kujala J, Hämäläinen L, Timmermann L, Schnitzler A, Salmelin R (2001) Dynamic imaging of coherent sources: studying neural interactions in the human brain. Proc Natl Acad Sci U S A 98: 694-699.

Guderian S, Schott BH, Richardson-Klavehn A, Duzel E (2009) Medial temporal theta state before an event predicts episodic encoding success in humans. Proc Natl Acad Sci U S A 106:5365-5370.

Guitart-Masip M, Barnes GR, Horner A, Bauer M, Dolan RJ, Duzel E (2013) Synchronization of medial temporal lobe and prefrontal rhythms in human decision making. J Neurosci 33:442-451.

Hassabis D, Maguire EA (2007) Deconstructing episodic memory with construction. Trends Cogn Sci 11: 299-306.

Hassabis D, Kumaran D, Vann SD, Maguire EA (2007a) Patients with hippocampal amnesia cannot imagine new experiences. Proc Natl Acad Sci U S A 104:1726-1731.

Hassabis D, Kumaran D, Maguire, EA (2007b) Using imagination to understand the neural basis of episodic memory. J Neurosci 27:14365-14374.

Jeewajee A, Lever C, Burton S, O'Keefe J, Burgess N (2008) Environmental novelty is signaled by reduction of the hippocampal theta frequency. Hippocampus 18:340-348.

Joyce MKP, Barbas H (2018). Cortical connections position primate area 25 as a keystone for interoception, emotion, and memory. J Neurosci 38:1677-1698.

Kaplan R, Bush D, Bonnefond M, Bandettini PA, Barnes GR, Doeller CF, Burgess N (2014) Medial prefrontal theta phase coupling during spatial memory retrieval. Hippocampus 24:656-665.

Krieger-Redwood K, Teige C, Davey J, Hymers M, Jefferies E (2015) Conceptual control across modalities: graded specialisation for pictures and words in inferior frontal and posterior temporal cortex. Neuropsychologia 76:92-107.

Kuperman V, Stadthagen-Gonzalez H, Brysbaert M (2012) Age-of-acquisition ratings for 30,000 English words. Behav Res Methods 44:978-990.

Kwan D, Carson N, Addis DR, Rosenbaum RS (2010) Deficits in past remembering extend to future imagining in a case of developmental amnesia. Neuropsychologia 48:3179-3186.

Kurczek J, Wechsler E, Ahuja S, Jensen U, Cohen NJ, Tranel D, Duff M (2015) Differential contributions of hippocampus and medial prefrontal cortex to self-projection and self-referential processing. Neuropsychologia 73:116-126.

Lega BC, Germi J, Rugg M (2017) Modulation of oscillatory power and connectivity in the human posterior cingulate cortex supports the encoding and retrieval of episodic memories. J Cogn Neurosci 29:1415-1432.

Lega BC, Jacobs J, Kahana M (2012) Human hippocampal theta oscillations and the formation of episodic memories. Hippocampus 22:748-761.

Lesting J, Daldrup T, Narayanan V, Himpe C, Seidenbecher T, Pape HC (2013) Directional theta coherence in prefrontal cortical to amygdalo-hippocampal pathways signals fear extinction. PLoS One 8:e77707.

Lewis G, Poeppel D (2014) The role of visual representations during the lexical access of spoken words. Brain Lang 134:1-10.

Maguire EA, Mullally SL (2013) The hippocampus: a manifesto for change. J Exp Psychol Gen 142:1180-1189.

Matsumoto JY, Stead M, Kucewicz MT, Matsumoto AJ, Peters PA, Brinkmann BH, Marsh WR, Meyer FB, Worrell GA (2013) Network oscillations modulate interictal epileptiform spike rate during human memory. Brain 136:2444-2456.

McCormick C, Ciaramelli E, De Luca F, Maguire EA (2018) Comparing and contrasting the cognitive effects of hippocampal and ventromedial prefrontal cortex damage: A review of human lesion studies. Neuroscience 374:295–318.

Michelmann S, Bowman H, Hanslmayr S (2016) The temporal signature of memories: Identification of a general mechanism for dynamic memory replay in humans. PLoS Biol 14:e1002528.

Moran R, Pinotsis DA, Friston K (2013) Neural masses and fields in dynamic causal modeling. Front Comput Neurosci 7:57.

Moran RJ, Stephan KE, Seidenbecher T, Pape HC, Dolan RJ, Friston KJ (2009) Dynamic causal models of steady-state responses. Neuroimage 44:796-811.

Mullally SL, Maguire EA (2011) A new role for the parahippocampal cortex in representing space. J Neurosci 31:7441-7449.

Nieuwenhuis IL, Takashima A (2011) The role of the ventromedial prefrontal cortex in memory consolidation Behav Brain Res 218:325-334.

Nolte G (2003) The magnetic lead field theorem in the quasi-static approximation and its use for magnetoencephalography forward calculation in realistic volume conductors. Phys Med Biol 48:3637-3652.

Place R, Farovik A, Brockmann M, Eichenbaum H (2016) Bidirectional prefrontal-hippocampal interactions support context-guided memory. Nat Neurosci 19:992-994.

Rempel-Clower NL, Barbas H (2000) The laminar pattern of connections between prefrontal and anterior temporal cortices in the rhesus monkey is related to cortical structure and function. Cereb Cortex 10:851-865.

Schacter DL, Addis DR (2007) The cognitive neuroscience of constructive memory: remembering the past and imagining the future. Philos Trans R Soc B 362:773-786.

Scheeringa R, Fries P, Petersson KM, Oostenveld R, Grothe I, Norris DG, Hagoort P, Bastiaansen MCM (2011) Neuronal dynamics underlying high- and low-frequency EEG oscillations contribute independently to the human BOLD signal. Neuron 69:572-583.

Scoville WB, Milner B (1957) Loss of recent memory after bilateral hippocampal lesions. J Neurol Neurosurg Psychiatry 20:11-21.

Sederberg PB, Schulze-Bonhage A, Madsen JR, Bromfield, EB, McCarthy DC, Brandt A, Tully MS, Kahana MJ (2007) Hippocampal and neocortical gamma oscillations predict memory formation in humans. Cereb Cortex 17:1190-1196.

Stephan KE, Penny WD, Daunizeau J, Moran RJ, Friston KJ (2009) Bayesian model selection for group studies. Neuroimage 46:1004-1017.

742 Turner MS, Cipolotti L, Yousry TA, Shallice T (2008) Confabulation: damage to a specific inferior
743 medial prefrontal system. Cortex 44:637-648.
744 Tzourio-Mazoyer N, Landeau B, Papathanassiou D, Crivello F, Etard O, Delcroix, N, Mazoyer B, Joliot
745 M (2002) Automated anatomical labeling of activations in SPM using a macroscopic
746 anatomical parcellation of the MNI MRI single-subject brain. Neuroimage 15:273-289.
747 van Heuven WJB, Mandera P, Keuleers E, Brysbaert M (2014) Subtlex-UK: a new and improved word
748 frequency database for British English. Q J Exp Psychol 67:1176-1190.
749 van Kesteren MT, Beul SF, Takashima A, Henson RN, Ruiter DJ, Fernandez G (2013) Differential roles
750 for medial prefrontal and medial temporal cortices in schema-dependent encoding: from
751 congruent to incongruent. Neuropsychologia 51:2352-2359.
752 Varela C, Kumar S, Yang JY, Wilson MA (2014) Anatomical substrates for direct interactions between
753 hippocampus, medial prefrontal cortex, and the thalamic nucleus reuniens. Brain Struct
754 Funct 219:911-929.
755 Vigliocco G, Kousta ST, Della Rosa PA, Vinson DP, Tettamanti M, Devlin JT, Cappa SF (2014) The
756 neural representation of abstract words: the role of emotion. Cereb Cortex 24:1767-1777.
757 Warren DE, Jones SH, Duff MC, Tranel D (2014) False recall is reduced by damage to the
758 ventromedial prefrontal cortex: implications for understanding the neural correlates of
759 schematic memory. J Neurosci 34:7677-7682.
760 Warriner AB, Kuperman V, Brysbaert M (2013) Norms of valence, arousal, and dominance for 13,915
761 English lemmas. Behav Res Methods 45:1191-1207.
762 Xiao D, Zikopoulos B, Barbas H (2009) Laminar and modular organization of prefrontal projections to
763 multiple thalamic nuclei. Neuroscience 161:1067-1081.
764 Zeidman P, Maguire EA (2016) Anterior hippocampus: the anatomy of perception, imagination and
765 episodic memory. Nature Rev Neurosci 17:173-182.
766 Zeidman P, Mullally SL, Maguire EA (2015) Constructing, perceiving, and maintaining scenes:
767 hippocampal activity and connectivity. Cereb Cortex 25:3836-3855.
768
769
770
771